

High output nanogenerator based on assembly of GaN nanowires

This article has been downloaded from IOPscience. Please scroll down to see the full text article.

2011 Nanotechnology 22 475401

(<http://iopscience.iop.org/0957-4484/22/47/475401>)

View [the table of contents for this issue](#), or go to the [journal homepage](#) for more

Download details:

IP Address: 130.207.50.192

The article was downloaded on 03/11/2011 at 15:32

Please note that [terms and conditions apply](#).

High output nanogenerator based on assembly of GaN nanowires

Long Lin^{1,3}, Chen-Ho Lai^{1,2,3}, Youfan Hu¹, Yan Zhang¹,
Xue Wang¹, Chen Xu¹, Robert L Snyder¹, Lih-J Chen² and
Zhong Lin Wang¹

¹ School of Materials Science and Engineering, Georgia Institute of Technology, Atlanta, GA 30332, USA

² Department of Materials Science and Engineering, National Tsing-Hua University, Hsin-Chu, Taiwan 30013, Republic of China

E-mail: robert.snyder@mse.gatech.edu, ljchen@mx.nthu.edu.tw and zlwang@gatech.edu

Received 28 July 2011, in final form 8 October 2011

Published 2 November 2011

Online at stacks.iop.org/Nano/22/475401

Abstract

GaN nanowires (NWs) were synthesized through a vapor–liquid–solid (VLS) process. Based on structural analysis, the *c*-axis of the NW was confirmed to be perpendicular to the growth direction. Nanogenerators (NGs) fabricated by rational assembly of the GaN NWs produced an output voltage up to 1.2 V and output current density of $0.16 \mu\text{A cm}^{-2}$. The measured performance of the GaN NGs was consistent with the calculations using finite element analysis (FEA).

(Some figures may appear in colour only in the online journal)

1. Introduction

Harvesting energy from our living environment is a very active research field for powering micro/nano-systems [1]. Nowadays, various approaches have been developed for solar cells [2–5], thermoelectric cells [6, 7], hydrogen fuel cells [8, 9], etc. Mechanical energy, such as vibrational energy, body movement, and heart beating, can serve as energy resources at any time and in any place. Recently, piezoelectric nanogenerators (NGs) [10–17] have been developed by taking advantage of the piezoelectric property of semiconductor nanostructures to convert mechanical energy into electric energy. NGs based on different kinds of nanomaterials have been demonstrated, including ZnO [10–16], GaN [17], and lead zirconate titanate (PZT) [18]. Owing to the large direct band gap, good thermal stability and high mobility [19], GaN has shown outstanding optoelectronic properties, and reveals great application potentials in many fields, but it has been rarely used for NGs especially with high output performance.

In this work, by utilizing rational assembly of GaN nanowires (NWs), we demonstrate the first NGs of GaN with high output performance. The NG was fabricated by an assembly of GaN NWs on a flexible substrate, and an output

voltage up to 1.2 V was achieved. The measured output voltage was consistent with numerical calculation using finite element analysis (FEA).

2. Experimental section

The growth of GaN NWs was based on a promotion of previously described vapor–liquid–solid (VLS) processes [17]. First, a 2 nm thick Ni film was deposited on the (001) Si substrate by magnetron sputtering. This thin metal film served as a catalyst for the growth of GaN NWs. Then, the as-prepared substrate was placed in the middle of an alumina boat, while gallium metal was placed on both ends of the boat as a Ga source. The placement of Ga metal on both ends could effectively prevent oxidation of the product. Finally, the whole boat was put in the middle of a horizontal tube furnace and was evacuated to a pressure below 8×10^{-3} Torr to remove oxygen and moisture. With an ammonia gas flow of 30 sccm (standard cubic centimeters per minute), the furnace was heated to 900 °C and then kept at 900 °C for 30 min. The GaN NWs were formed due to the chemical reaction at high temperature between Ga metal and NH_3 . Compared to the previous work using sapphire substrate and metal–organic chemical vapor deposition (MOCVD) for depositing GaN thin

³ These two authors contributed equally to this work.

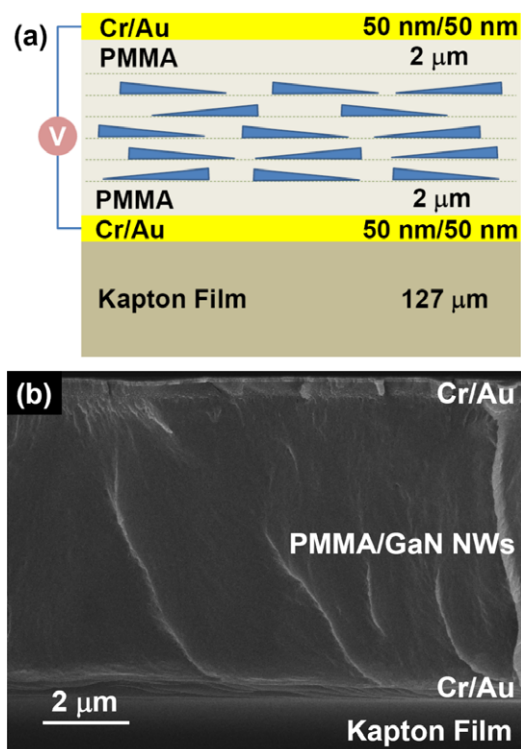


Figure 1. (a) Schematic illustration of the structure of the GaN NG. (b) Cross-sectional SEM image showing the composite structure of the GaN NG.

film [17], the method in this work was significantly more cost effective. Scanning electron microscopy (SEM) (LEO 1530), transmission electron microscopy (TEM) (Hitachi 2000 and JEOL 4000EX), and energy-dispersive x-ray spectroscopy

(EDS) were utilized to characterize the structure of the GaN NWs.

NGs were fabricated using the GaN NWs employing an approach previously demonstrated for conical shaped ZnO NWs [15]. As shown in figure 1, the GaN NG was composed of a multi-layer of NWs infiltrated with polymethyl methacrylate (PMMA), which was sandwiched by two metal electrodes of Cr/Au. In the first step, the Cr/Au electrode was deposited on a Kapton film (DuPont 500 HN, 127 μm) by electron beam evaporation. Then, a layer of PMMA was deposited on this electrode by spin-coating. In the next step, the GaN NWs were suspended in ethanol by an ultrasonic wave and then dispersed on the substrate. Another thinner layer of PMMA was spin-coated after the ethanol had been evaporated from the substrate. After five cycles of GaN NWs and PMMA alternating deposition, another thicker layer of PMMA was spin-coated on. Finally, the top electrode of Cr/Au was deposited on the composite structure to serve as the top electrode. The effective size of the NG was 5 mm \times 5 mm.

3. Results and discussion

An SEM image of the as-synthesized GaN NWs is shown in figure 2(a). It can be observed that the length of the NWs ranges from 10 to 20 μm , and the diameter varies from 100 to 500 nm. From the inset high magnification image, it was shown that the cross section of the NWs is a triangle. The aspect ratio of the NWs may vary due to different parameters in the growth process, such as temperature, flow rate of carrier gas, and relative position of the substrate in the tube furnace. Figure 2(b) shows the EDS analysis of the NWs, which indicates the main composition of the NWs is GaN, and the copper signal would most probably come from the background

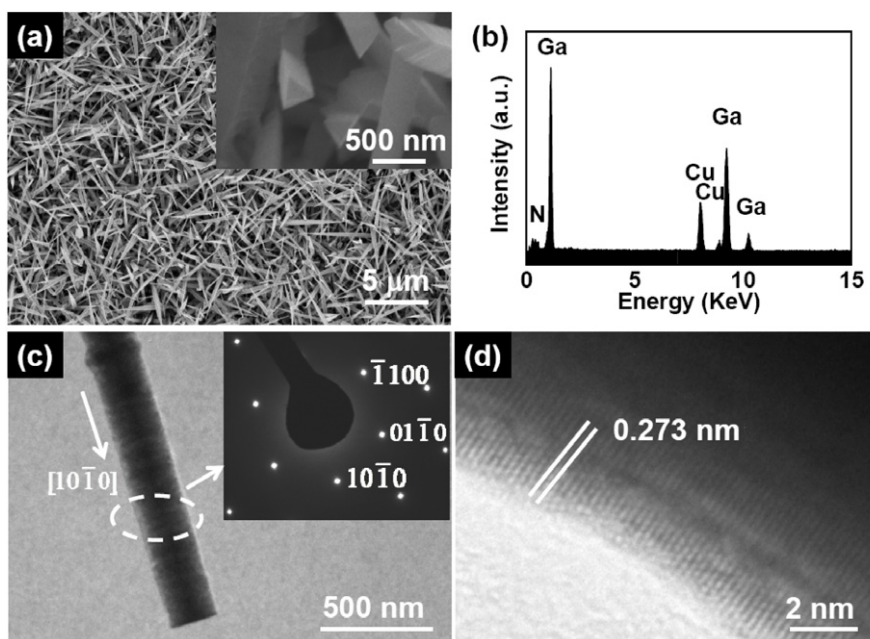


Figure 2. Crystal structure and composition of the as-synthesized GaN NWs. (a) Top-view SEM image of the GaN NWs. The inset is a high magnification SEM image showing the triangular cross section of the NW. (b) EDS analysis of the GaN NWs. (c) High magnification TEM image of a single GaN NW, the inset is the corresponding selected-area diffraction pattern. (d) High resolution TEM image of a single GaN NW.

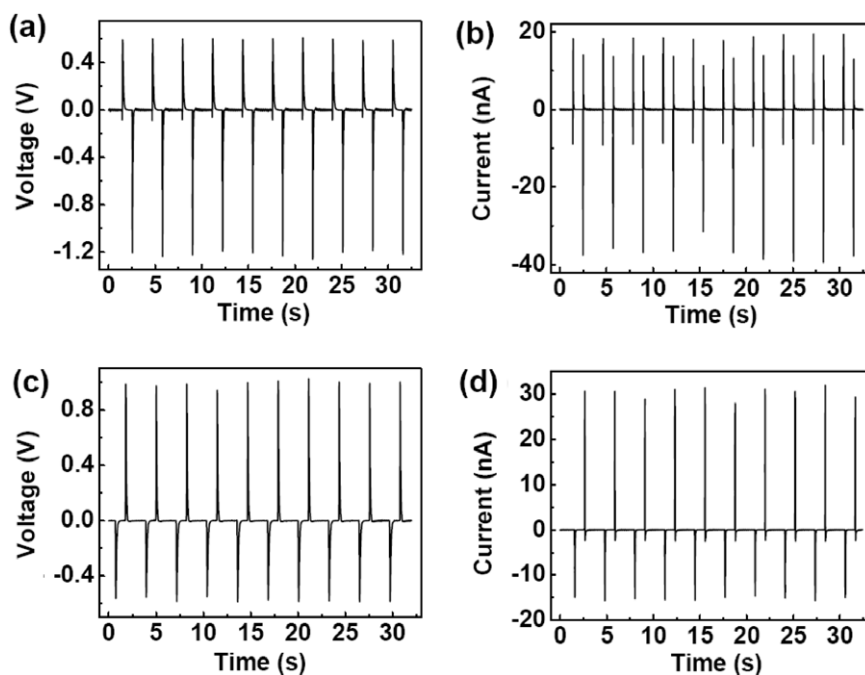


Figure 3. (a) Output voltage of the NG with forward connection. (b) Output current of the NG with forward connection. (c) Output voltage of the NG with reverse connection. (d) Output current of the NG with reverse connection.

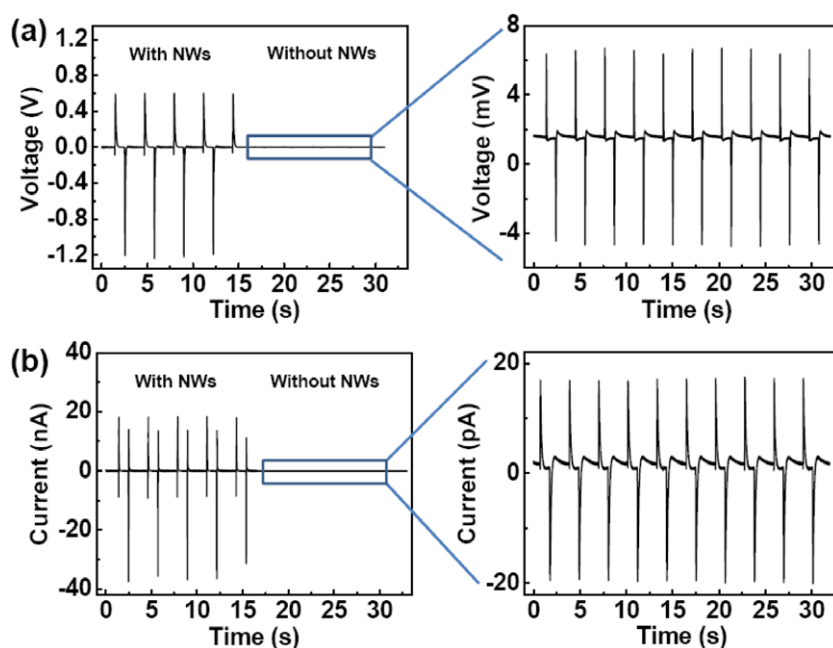


Figure 4. Comparison of electrical measurement between normal NG devices and the devices without the GaN NWs. (a) Comparison of output voltage between normal NG devices and the devices without the GaN NWs. The right image is the output voltage of devices without GaN NWs at high magnification. (b) Comparison of output current between normal NG devices and the devices without the GaN NWs. The right image is the output current of devices without GaN NWs at high magnification.

of the copper grid. Based on the TEM image in figure 2(c) and the inset diffraction pattern, the growth orientation of the NW is $\langle 10\bar{1}0 \rangle$. This orientation is perpendicular to the c axis of the NWs, which is consistent with a previous study of GaN NWs [17]. The high resolution TEM image of the GaN NWs is shown in figure 2(d). The planar distance of the crystal planes

which are perpendicular to the direction of the NW is measured to be 0.273 nm, which further confirmed that the orientation of the NWs is along the $\langle 10\bar{1}0 \rangle$ direction.

For the measurement of electrical output, the as-fabricated GaN NG was attached to a flexible polystyrene (PS) substrate and then an external force was applied to bend the PS substrate

with a linear motor. For simplicity, it was assumed that the NWs only experienced compressive strain due to a much larger thickness of the PS substrate relative to that of the assembled NG. The triangular cross section, the crystal structure and the orientation of the NWs play very important roles in the NG's high output performance. A piezoelectric polarization across the top and bottom electrodes was produced when the NG was bent (to be discussed in figure 5). The potential difference will drive the electrons flowing in the external circuit, from the bottom electrode to the top electrode. When the applied force is withdrawn, the strain in the NWs as well as the potential difference between the two electrodes disappears. The accumulated electrons at the top electrode will flow back, and thus an ac output signal is produced [13]. This working mechanism is similar to that of our previously demonstrated ZnO NG [15], while the major difference is that the overall component of the c axis across the thickness of the NG results from the triangular cross section of the NW, rather than the conical shape of the NW in the ZnO NG.

The typical electrical output of the assembled NG is shown in figures 3(a) and (b). The measured output voltage and the output current could be up to 1.2 V and 40 nA, respectively. The corresponding output current density was $0.16 \mu\text{A cm}^{-2}$. For verification purposes, we also measured the output of the NG with a reverse connection to the external measuring circuit. It can be seen in figures 3(c) and (d) that the sign of the output signal of the reverse connected NG was just opposite to that of the forward connected one. Thus it was confirmed that most of the measured signal came from NGs rather than from environmental noise [20].

To further confirm the validity of measurement and exclude the possible effect of environmental noise or systematic errors, we conducted a control experiment comparing the electrical output of the NG devices without the GaN NWs to that of the normal NG devices. As could be observed in figures 4(a) and (b), the output voltage and output current of the devices without the GaN NWs were two orders and three orders of magnitude lower than those of the devices with the GaN NWs, respectively. Therefore, it was ensured that possible noise in this measurement system could be neglected.

Though the performance of the GaN NG was not higher than that of the previously demonstrated ZnO NG with similar structure, it was still more promising in some specific cases. First, an ultimate goal for our NG projects was to develop self-powered nano-systems. GaN was widely used for optoelectronic devices such as light-emitting diodes and quantum well lasers [21]. The GaN-based NG had potential applications for fabricating hybrid devices which could harvest energy from the environment and drive functional parts of the devices. Second, defects such as oxygen vacancies were inevitable during the synthesis of ZnO NWs, which was a major drawback of the ZnO NG due to the screening effect from high carrier density, while the unintentionally doped GaN NWs were relatively free of such defects, and thus much higher performance could be anticipated if advanced techniques such as MOCVD or molecular beam epitaxy (MBE) were employed to grow the GaN NWs with higher qualities.

To understand the mechanism of harvesting energy with this structure, we calculated the potential across the thickness

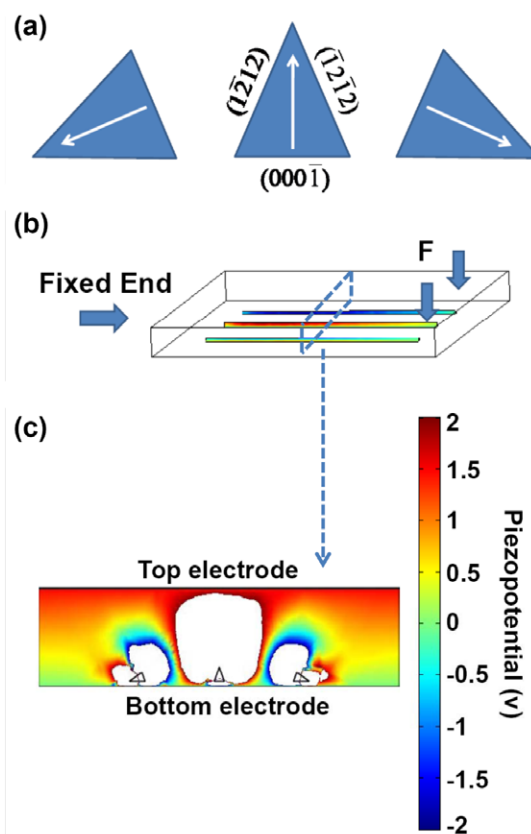


Figure 5. (a) Schematic of the cross section of the NWs with three possible orientations. The arrows show the direction of c axis in each NW. (b) Schematic model showing the setup for numerical calculation of the potential across the thickness of the NG. The entire structure is like a one-end-fixed (left-hand side) beam, with a transverse force applied at the free end. (c) Taking a cross section at the midpoint of the NWs, the calculated potential difference between the top and bottom electrodes of a NG is presented. The blank region close to the NWs indicates that the local potential is over the range of the color display.

of the NG structure with a simple model using finite element analysis (FEA), as shown in figures 5(a) and (b). The three side surfaces of the GaN NW were $(000\bar{1})$, $(\bar{1}2\bar{1}1)$, and $(\bar{1}2\bar{1}1)$ [22]. The NG structure is a 'capacitor-like' plate structure in which the GaN NWs and PMMA serve as a composite 'dielectric medium'. Since the cross section of the NW is an isosceles triangle, we assume that each of its three side surfaces has an equal possibility to lie flat on the substrate. Based on this assumption, three NWs with different orientations were placed in a unit cell. The whole structure was considered as a cantilever with its one end being fixed and a periodic force of 40 MPa being applied at the top edge of the other end. Lipmann theory [23] was used to calculate the piezopotential introduced inside the NW. For simplicity of the simulation, the NWs were taken to have a uniform size of $19.5 \mu\text{m}$ in length. The dimension of the unit cell for the simulation was $20 \mu\text{m} \times 7.5 \mu\text{m} \times 2 \mu\text{m}$. In this case, the density of NWs in the unit cell was $20\,000 \text{ NWs mm}^{-2}$, which matches the density of NWs in the realized structure. The material constants of the GaN NW were taken as $a = 0.3189 \text{ nm}$, $c = 0.5185 \text{ nm}$,

$C_{11} = 390$ GPa, $C_{12} = 145$ GPa, $C_{13} = 106$ GPa, $C_{33} = 398$ GPa, $C_{44} = 105$ GPa, piezoelectric constants $e_{15} = e_{31} = -0.49$ C m⁻², $e_{33} = 0.73$ C m⁻², relative dielectric constants $k_{11} = k_{22} = 9.28$, $k_{33} = 10.01$ [24], and the density of GaN $\rho = 6150$ kg m⁻³. For the purpose of simplicity, the NWs were assumed to be insulating.

The calculation result is shown in figure 5(c). It is shown that the calculated potential across the thickness of this structure is 1.5 V. The measured output voltage of 1.2 V was consistent with this calculation result. The measured output voltage was a little lower than the calculation result and this was probably due to the screening effect of the GaN NWs, since the GaN NWs were not ideally insulating [25].

4. Conclusion

In summary, we have successfully fabricated high output NGs using GaN NWs with triangular cross section. The GaN NW shows an orientation of $\langle 10\bar{1}0 \rangle$ along the NW direction, with the c axis perpendicular to the NW. The as-fabricated NG is a ‘capacitor-like’ plate structure, in which GaN NWs and PMMA serve as ‘dielectric media’. The output voltage and output current density could be up to 1.2 V and $0.16 \mu\text{A cm}^{-2}$, respectively. The calculated piezopotential is consistent with the measured output. This study shows that GaN NWs can be a good candidate for fabricating high output NGs for driving small electric devices.

Acknowledgments

We are grateful to BES DOE, NSF, and DARPA for their support and to Drs Chi-Te Huang, Yong Ding, Ya Yang, and Cheng-Ying Chen for their help and stimulating discussions.

References

- [1] Wang Z L 2008 *Adv. Funct. Mater.* **18** 3553–67
- [2] Dresselhaus M S and Thomas I L 2001 *Nature* **414** 332–7
- [3] Huynh W U, Dittmer J J and Alivisatos A P 2002 *Science* **295** 2425–7
- [4] Tian B Z, Zheng X L, Kempa T J, Fang Y, Yu N F, Yu G H, Huang J L and Lieber C M 2007 *Nature* **449** 885–9
- [5] Law M, Greene L E, Johnson J C, Saykally R and Yang P D 2005 *Nature Mater.* **4** 455–9
- [6] Boukai A I, Bunimovich Y, Kheli J T, Yu J K, Goddard W A III and Heath J R 2008 *Nature* **451** 168–71
- [7] Poudel B et al 2008 *Science* **320** 634–8
- [8] Steele B C H and Heinzl A 2001 *Nature* **414** 345–52
- [9] Schlapbach L 2009 *Nature* **460** 809–11
- [10] Wang Z L and Song J H 2006 *Science* **312** 242–6
- [11] Wang X D, Song J H, Liu J and Wang Z L 2007 *Science* **316** 102–5
- [12] Qin Y, Wang X D and Wang Z L 2008 *Nature* **451** 809–13
- [13] Yang R S, Qin Y, Dai L M and Wang Z L 2009 *Nature Nanotechnol.* **4** 34–9
- [14] Choi M-Y, Choi D, Jin M-J, Kim I, Kim S-H, Choi J-Y, Lee S Y, Kim J M and Kim S W 2009 *Adv. Mater.* **21** 2185–9
- [15] Hu Y F, Zhang Y, Xu C, Zhu G and Wang Z L 2010 *Nano Lett.* **10** 5025–31
- [16] Hu Y F, Zhang Y, Xu C, Lin L, Snyder R L and Wang Z L 2011 *Nano Lett.* **11** 2572–7
- [17] Huang C-T, Song J H, Lee W-F, Ding Y, Gao Z Y, Hao Y, Chen L-J and Wang Z L 2010 *J. Am. Chem. Soc.* **132** 4766–71
- [18] Chen X, Xu S Y, Yao N and Shi Y 2010 *Nano Lett.* **10** 2133–7
- [19] Huang Y, Duan X F, Cui Y and Lieber C M 2002 *Nano Lett.* **2** 101–4
- [20] Yang R S, Qin Y, Li C, Dai L M and Wang Z L 2009 *Appl. Phys. Lett.* **94** 022905
- [21] Park S-H and Chuang S-L 1998 *Appl. Phys. Lett.* **72** 3103–5
- [22] Qian F, Li Y, Gradečak S, Park H-G, Dong Y J, Ding Y, Wang Z L and Lieber C M 2008 *Nature Mater.* **7** 701–6
- [23] Gao Y F and Wang Z L 2007 *Nano Lett.* **7** 2499–505
- [24] Fonoberov V A and Balandin A A 2003 *J. Appl. Phys.* **94** 7178–86
- [25] Strite S and Morkoc H 1992 *J. Vac. Sci. Technol. B* **10** 1237–66